Title

Role of matrix metalloproteinase-9 in neurodevelopmental disorders and experience-dependent plasticity in Xenopus tadpoles.

Authors

Sayali Gore[1], Eric J. James[1], Lin-Chien Huang[2], Jenn J. Park[1], Andrea Berghella[1], Adrian Thompson[1], Hollis T. Cline[2], Carlos D. Aizenman[1*]

Affiliations

[1]Department of Neuroscience, Brown University, Providence, RI

[2]The Scripps Research Institute, La Jolla, CA

[*] Corresponding author:

Dr. Carlos Aizenman, Brown University, Department of Neuroscience – Box G-LN, Providence, RI 02912

T. (401) 863-6016, F. (401) 863-1074

Email: carlos_aizenman-stern@brown.edu

Carlos_Aizenman@brown.edu

Abstract

Matrix metalloproteinase-9 (MMP-9) is a secreted endopeptidase targeting extracellular matrix proteins, creating permissive environments for neuronal development and plasticity. Developmental dysregulation of MMP-9 is also associated with neurodevelopmental disorders (ND). Here we test the hypothesis that chronically elevated MMP-9 activity during early neurodevelopment is responsible for neural circuit hyperconnectivity observed after early exposure to valproic acid (VPA), a known teratogen associated with autism spectrum disorder in humans. In *Xenopus* tadpoles, VPA exposure results in excess local synaptic connectivity, disrupted social behavior and increased seizure susceptibility. We found that overexpressing MMP-9 in the brain copies effects of VPA on synaptic connectivity, and blocking MMP-9 activity pharmacologically or genetically reverses effects of VPA on physiology and behavior. We further show that during normal neurodevelopment MMP-9 levels are tightly regulated by neuronal activity and required for structural plasticity. These studies show a critical role for MMP-9 in both normal and abnormal development.

Introduction

Autism spectrum disorder (ASD) encompasses a highly heterogeneous set of neurodevelopmental conditions characterized by a complex behavioral phenotype and deficits in both social and cognitive functions. Over 100 gene mutations have been associated with ASD suggesting very different underlying etiologies(Betancur, 2011; Betancur & Coleman, 2013; Butler, 2018; Croft et al., 2011; Grove et al., 2019). This complex neurodevelopmental disorder, which is influenced by both genetic and environmental factors, results from profound changes in brain function and connectivity. The pathophysiology of ASD is often attributed to abnormal synaptic maturation and plasticity, defects in microcircuitry organization, disruption of the brain excitation to inhibition balance, local overconnectivity and long-range underconnectivity throughout the brain(Kumar et al., 2019; Markram & Markram, 2010). Even though some aspects of the etiology of ASD have been studied, how ASD-related behaviors arise from synaptic dysfunction and abnormal neural circuit development remain elusive. Studies in both humans(Bromley et al., 2013; Christensen et al., 2013) and animal models(Markram et al., 2008; Rodier et al., 1996; Roullet et al., 2010; Schneider et al., 2006; Schneider & Przewłocki, 2005) have shown that prenatal exposure to valproic acid (VPA), a common antiepileptic drug, results in a higher incidence of ASD in humans or ASD-like deficits in animals. In rodents, in utero exposure to VPA results in autistic-like behaviors in offspring; namely decreased socialization, increased repetitive behaviors, and hypersensitivity to sensory stimuli(Kataoka et al., 2013; Kim et al., 2011; Mehta et al., 2011; Moldrich et al., 2013). These behavioral deficits are accompanied by corresponding deficits in brain physiology, including increased local recurrent connectivity, synaptic activity, and decreased intrinsic neuronal excitability(Markram & Markram, 2010). Xenopus tadpoles when exposed to VPA have abnormal sensory-motor and schooling behavior which is accompanied by hyper-connected neural networks in the optic tectum, increased excitatory and inhibitory synaptic drive, elevated levels of

spontaneous synaptic activity and decreased neuronal intrinsic excitability(James et al., 2015). Consistent with these findings, VPA treated tadpoles also have increased seizure susceptibility and decreased acoustic startle habituation(James et al., 2015). VPA, a known histone-deacetylase inhibitor, causes these effects by hyperacetylation of gene promoters, and thus, by altering gene expression of various targets(Ghodke-Puranik et al., 2013; Terbach & Williams, 2009). Preliminary studies in Xenopus using microarrays identified MMP-9 upregulation as a potential downstream effector of VPA exposure, suggesting that dysregulation of this protein may be important for mediating effects of VPA.

MMP-9 is a secreted zinc-dependent extracellular endopeptidase that can cleave ECM and several cell surface receptors facilitating synaptic and circuit level reorganization(Ethell & Ethell, 2007; Niedringhaus et al., 2012; Reinhard et al., 2015). Early formation of proper synaptic connections and neural circuits is heavily regulated by the pericellular environment, and dysregulation of proteins important for extracellular matrix function could disrupt this process resulting in circuit abnormalities associated with ASD(Choi, 2018; Ferrer-Ferrer & Dityatev, 2018). During development, experience-dependent activity during critical periods can drive neural plasticity and MMP-9 plays an important role in this critical period plasticity(Murase et al., 2017; Oliveira-Silva et al., 2007; Reinhard et al., 2015; Spolidoro et al., 2012). Furthermore, MMP-9 is thought to play a role in adult neurogenesis and synaptic plasticity in the adult brain, and has been implicated in neural circuit formation(Fujioka et al., 2012; Peixoto et al., 2012; Pielecka-Fortuna et al., 2015; Wang et al., 2008).

Previous studies from the lab have utilized the Xenopus laevis tadpole CNS as a model for understanding the synaptic origin of neurodevelopmental disorders(James et al., 2015; Pratt & Khakhalin, 2013; Truszkowski et al., 2016). The optic tectum, a region in Xenopus CNS, receives converging inputs from multiple sensory modalities and is responsible for carrying out multisensory

integration(Deeg & Aizenman, 2011; Pratt & Aizenman, 2007, 2009). The retinotectal circuit and local circuits within the optic tectum are known to refine during development in an activity-dependent manner and mediate robust visually-guided behaviors that are very sensitive to abnormal circuit development(Dong et al., 2009; R. H. Lee et al., 2010), providing a strong link between neural circuit dysfunction and behavior and provide a robust model for understanding neurodevelopmental disorders at various levels of organization - from synapses to behavior. The present work investigates (1) whether upregulation of MMP-9 by whole-brain electroporation mimics electrophysiological effects induced by VPA, (2) whether downregulation of MMP-9 using a pharmacological agent or an antisense morpholino directed against MMP-9 rescues VPA-induced electrophysiological and behavioral effects, and (3) whether MMP-9 is required for activity dependent structural plasticity.

Results

MMP-9 overexpression increases spontaneous synaptic activity and network connectivity, an effect also observed after VPA exposure

Exposure to VPA increases spontaneous synaptic activity, network connectivity and excitability in the developing tectum in Xenopus(James et al., 2015). Previous microarray studies from the lab have shown that VPA exposure results striking alterations in gene expression, including a greater than two-fold increase in matrix metalloproteinase 9 (MMP-9). Here we validated this finding by performing qPCR on tectal samples of VPA-exposed tadpoles and found a several-fold increase in mRNA levels for MMP9 *[increase in MMP9 mRNA: 2.7±0.3 fold increase over control, n=3 replicates]*. This suggested the hypothesis that chronically elevated levels of MMP-9 may mediate some of the effects of VPA by promoting excess plasticity leading to local hyperconnectivity. Thus, we first tested whether overexpression of MMP-9 mimics the VPA-induced effects on synaptic connectivity and excitability in

the developing tectum. MMP-9 was overexpressed in tectal neurons using whole-brain electroporation, which results in expression in a small percent of tectal neurons(Haas et al., 2002). We performed whole-cell patch-clamp recordings from MMP-9-expressing tectal neurons using an *ex vivo* whole-brain preparation. One-way ANOVA showed significant differences in sEPSC between groups [sEPSCs frequency (events/s): $p = 0.002$, sIPSCs frequency (events/s): $p = 0.03$]. Post-hoc pairwise comparison indicated a significant increase in the frequency of sEPSCs [*sEPSCs frequency (events/s): GFP control, 1.37 ± 0.39, n = 11; MMP-9 transfected, 6.74 ± 1.54, n = 15; MMP-9 non-transfected, 2.92 ± 0.63, n = 19; p(GFP control and MMP-9 transfected) = 0.004; p(MMP-9 non-transfected and MMP-9 transfected) = 0.02)*] and sIPSCs [*sIPSCs frequency (events/s): GFP control, 5.22 ± 0.97, n = 11; MMP-9 transfected, 8.09 ± 0.73, n = 13; MMP-9 non-transfected, 6.34 ± 0.52, n = 15; p(GFP control and MMP-9 transfected) = 0.03; p(MMP-9 non-transfected and MMP-9 transfected) = 0.25)*] in the transfected MMP-9 overexpressing tectal cells compared with GFP controls and non-transfected neighbors (Fig. 1 A,B). There were no significant differences in the sEPSC amplitude [*sEPSCs amplitude (pA): GFP control, 5.53 ± 0.56, n = 11; MMP-9 transfected, 6.18 ± 0.33, n = 15; MMP-9 non-transfected, 6.51 ± 0.99, n = 19; p = 0.45)*] or sIPSCs amplitude [*sIPSCs amplitude (pA): GFP control, 5.22 ± 0.33, n = 11; MMP-9 transfected, 5.99 ± 0.46, n = 13; MMP-9 non-transfected, 4.93 ± 0.43, n = 15; p = 0.19*] (Fig. 1C), consistent with VPA-induced effects (James at al, 2015). Increased synaptic transmission observed in MMP-9 overexpressing tectal neurons is consistent with dysfunctional synaptic pruning of sensory and local synaptic connections during development. Various theories of ASD and other neurodevelopmental disorders suggest that hyperconnected and hyperexcitable networks are the hallmarks of these disorders(Supekar et al., 2013; Takarae & Sweeney, 2017). In the developing Xenopus tectum, spontaneous barrages of recurrent synaptic activity are often used as a measure of intra-tectal connectivity and network excitability(James et al., 2015; Pratt & Aizenman, 2007). To gather

more information about the tectal connectivity and excitability, we counted the number of spontaneous recurrent barrages occurring in MMP-9 overexpressing tectal cells as well as from GFP control cells. Increased number of spontaneous recurrent barrages were observed in both transfected and non-transfected cells from MMP-9 overexpressing animals, compared to GFP controls, indicating persistent local connectivity which usually is pruned during development(Pratt et al., 2008) [*Mean number of barrages/min: GFP control, 0.1 ± 0.1, n = 11; MMP-9 transfected, 1.13 ± 0.37, n = 15; MMP-9 non-transfected, 1.10 ± 0.40, n = 19*] (Fig. 1D). The increased amount of barrage activity in non-transfected neurons, indicates that a small number of MMP-9-overexpressing cells are also sufficient to drive enhanced activity in the whole tectal network.

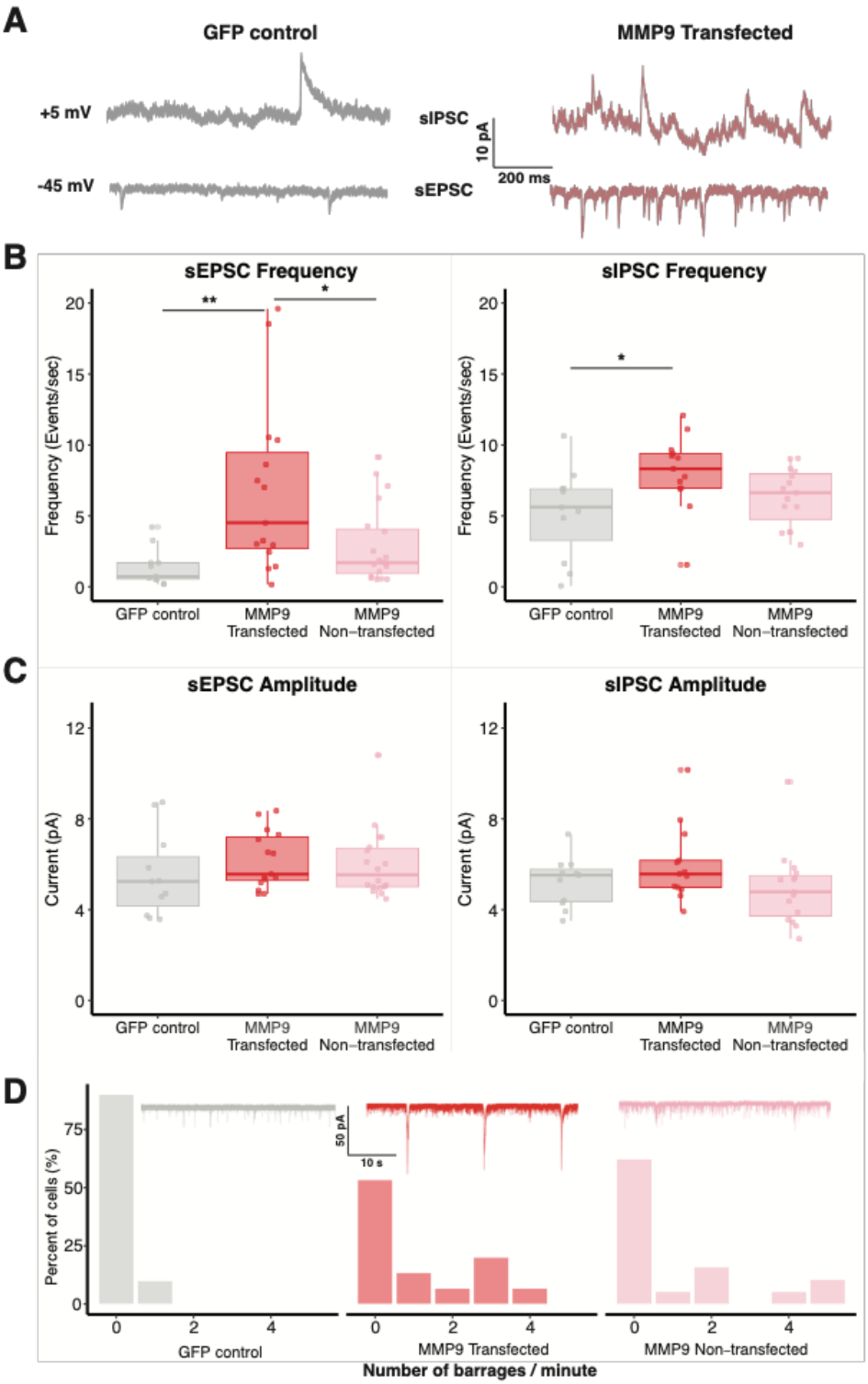

Figure 1: MMP-9 overexpression increases spontaneous synaptic activity and network connectivity

A. Representative sEPSCs and sIPSCs recorded at -45 mV and +5 mV, respectively, from control and MMP-9 transfected cells. **B.** Boxplots showing frequency of sEPSCs and sIPSCs for GFP control, MMP-9 transfected and MMP-9 non-transfected groups. The sEPSC and sIPSC frequencies are significantly enhanced in the MMP-9 transfected cells in comparison to the GFP control. Each dot represents data from one cell, the box represents median and interquartile range (IQR) and whiskers represent the range of data. **C.** Box plot showing sEPSC and sIPSC amplitudes for each group. The sEPSC and sIPSC amplitudes do not vary significantly between control, MMP-9 transfected and MMP-9 non-transfected groups. Data are represented as median ± IQR. **D.** Histogram showing relative barrage frequency for each group. The inset shows representative traces of barrages from each experimental group. MMP-9 transfected and non-transfected groups showed higher number of barrages (recorded at -45mV) than the GFP control group. * $p < 0.05$, ** $p < 0.005$.

Pharmacological inhibition of MMP-9 rescues VPA-induced effects

In order to confirm whether MMP-9 upregulation mediates the neurodevelopmental effects of VPA exposure, we tested whether downregulation of MMP-9 by introduction of a pharmacological inhibitor of MMP-9 (3μM SB-3CT) would rescue VPA-induced effects. The sEPSC frequency was significantly different across different treatments [*sEPSC frequency (events/s): p = 0.02*]. Consistent with prior observations, we observed a significant increase in the frequency of sEPSCs in the VPA group compared to the control. Addition of SB-3CT to VPA resulted in a reversal of the VPA-induced increase in sEPSC frequency, while SB-3CT alone did not show any significant effect of sEPSC frequency [*sEPSC frequency (events/s): control, 3.13± 0.48, n = 14; VPA, 6.78 ± 1, n = 21; VPA + SB-3CT, 4.3 ± 0.67, n = 22; SC-3CT, 4.46 ± 1.19, n = 11, P(control and VPA) = 0.004; P(VPA and VPA+SB-3CT) = 0.02)*] (Fig. 2A, B). There were no significant differences in sEPSC amplitude [*sEPSC amplitude (pA): control, 5.27 ± 0.36, n = 14; VPA, 5.83 ± 0.35, n = 21; VPA + SB-3CT, 5.94 ± 0.22, n = 22; SC-3CT, 5.11 ± 0.41, n = 11; p = 0.24)*] (Fig. 2C). We further assessed changes in local excitatory connectivity by measuring evoked synaptic recurrent activity by electrically stimulating the optic chiasm using a bipolar stimulating electrode, and measuring the total charge during a time window which consists of predominantly recurrent activity(Pratt et al., 2008). One-way ANOVA showed significant differences across treatments for evoked responses [*Total charge (pA.sec): p = 0.03*]. We observed that maximal excitatory responses were elevated in VPA-treated tadpoles compared to the control group; and this effect was reversed in the VPA + SB-3CT group [*Total charge (pA.sec): control, 1160.61 ± 521.17, n = 8; VPA, 4163.43 ± 574.77, n = 16; VPA + SB-3CT, 1780.89 ± 479.29, n = 5; SC-3CT, 2655.15 ± 718.41, n = 13; p(control and VPA) = 0.01; p(VPA and VPA+SB-3CT) = 0.03)*] (Fig. 2D). Increased number of spontaneous recurrent barrages were observed in the VPA-reared tadpoles, compared to the GFP control; an effect rescued when VPA-rearing media was supplemented with SB-3CT [*Number of*

barrages: control, 0.5 ± 0.19, n = 14; VPA, 1.19 ± 0.31, n = 21; VPA+SB-3CT, 0.59 ± 0.19, n = 22; SB-3CT, 0.36 ± 0.13, n = 11] (Fig. 2E). These data suggest that pharmacological inhibition of MMP-9 reverses increases in excitatory transmission observed in VPA treated animals, but has no effects on untreated controls, suggesting that basal MMP-9 levels are low.

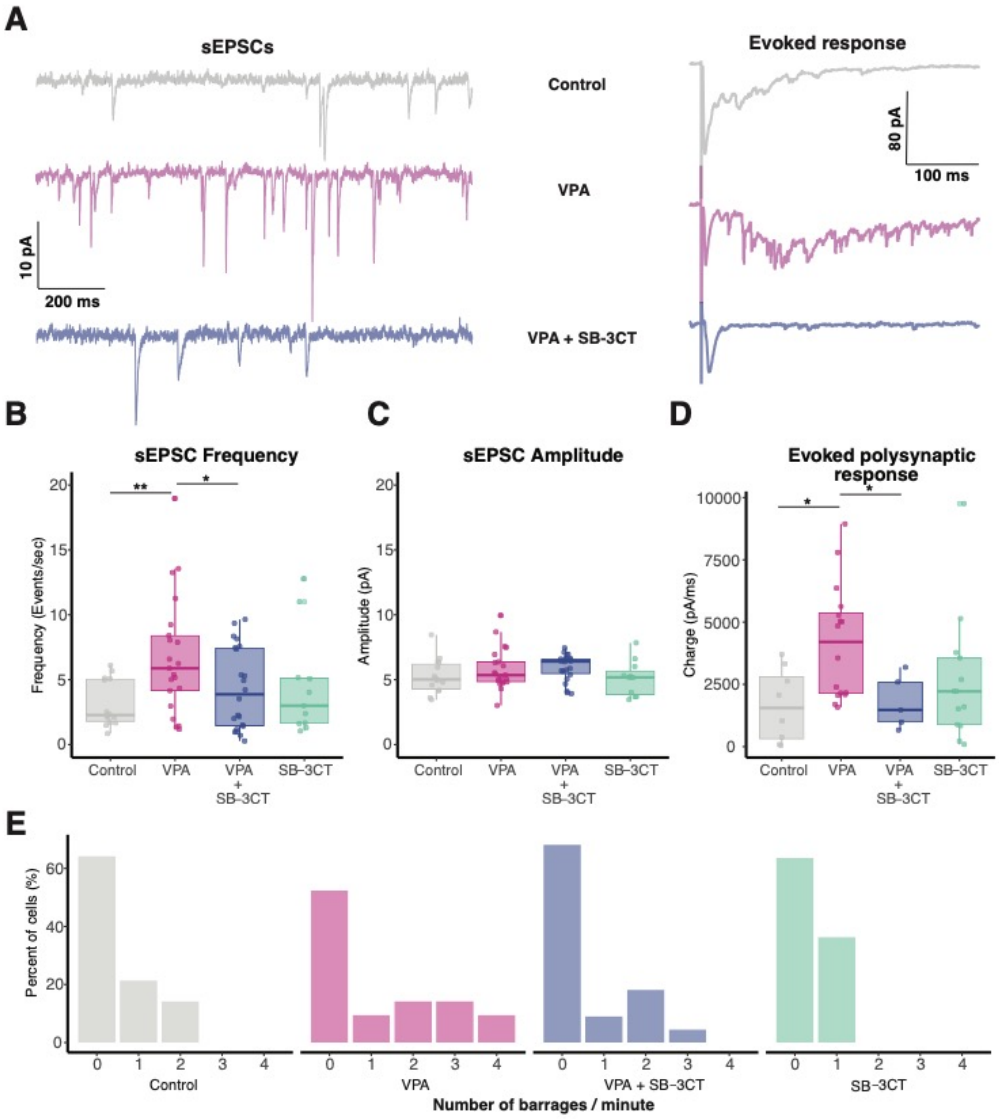

Figure 2: Pharmacological inhibition of MMP-9 rescues VPA-induced effects on synaptic transmission. Representative sEPSCs (left) and evoked response (right) form control, VPA and VPA + SB-3CT treated animals. **B.** Boxplots showing frequency of sEPSCs for control, VPA, VPA + SB-3CT and SB-3CT alone groups. Frequency of sEPSCs are significantly enhanced in VPA group, an effect rescued by addition of SB-3CT. SB-3CT alone does not have any significant effect on sEPSC frequency. Data are represented as median ± IQR. **C.** Boxplots showing sEPSCs amplitude for each group. sEPSC amplitude does not change significantly between control and treatment animals. Data are represented as median ± IQR. **D.** Boxplot showing total charge from evoked synaptic response over a 100 ms window for each group. Total charge from evoked synaptic response is significantly higher in VPA treated animals and this effect is rescued in the presence of SB-3CT. Data are represented as median ± IQR. **E.** Histogram showing relative barrage frequency for each group. Higher number of barrages are observed for VPA treated animals than in any other group. * $p < 0.05$, ** $p < 0.005$.

Morpholino targeted against MMP-9 rescues VPA-induced effects

As an alternative manipulation, we genetically downregulated levels of MMP-9 using an antisense morpholino oligo (MO) targeted against MMP-9 to test whether we could reverse VPA-induced effects. Whole-brain electroporation of the anti-MMP-9 MO, resulted in a significant decrease in endogenous MMP-9 levels when compared to the scrambled control MO (*Relative MMP-9 levels for MMP-9 MO/ Control MO, 0.72 ± 0.048, n = 5, p = 0.004*) (Fig 3A)**.** As an alternative measure for MO effectiveness, we overexpressed an MMP-9 construct containing a FLAG tag, and found that the MMP-9 MO could decrease overexpression levels (not shown). We observed a significant decrease in the frequency of sEPSCs in VPA+MMP-9 MO group compared to the VPA+control MO group suggesting that addition of MMP-9 MO in the presence of VPA rescues VPA-induced effects (Fig. 3B). In a separate set of experiments, electroporation of MMP-9 MO alone on untreated animals did not have any effect on sEPSC frequency when compared to control MO (Fig. 3C). [*sEPSC frequency (events/s): VPA+control MO, 5.99 ± 0.79, n = 9; VPA+MMP-9 MO, 1.55 ± 0.28, n = 10; control MO, 6.09 ± 1.27, n = 11; MMP-9 MO, 6.55 ± 1.33, n = 18, p(VPA+control MO and VPA+MMP-9 MO) < 0.0001 ; p (control MO and MMP-9MO) = 0.81*]. There were no significant differences in sEPSC amplitude [*VPA+control MO, 6.75 ± 0.57, n = 9; VPA+MMP-9 MO, 6.3 ± 0.51, n = 10; control MO, 6.57 ± 0.52, n = 11; MMP-9 MO, 6.73 ± 0.61, n = 18, p(VPA+control MO and VPA+MMP-9 MO) = 0.61; p (control MO and MMP-9 MO) = 0.60*] (Fig. 3C). We next examined changes in local excitatory connectivity by measuring evoked synaptic recurrent activity by electrically stimulating the optic chiasm. We observed that maximal excitatory responses were significantly reduced in the VPA+MMP-9 MO group in comparison to the VPA+control MO group [*Total charge (pA.sec): VPA+control MO, 14792 ± 2454.59, n = 9; VPA+MMP-9 MO, 2752.9 ± 390.4, n = 10, p (VPA+control MO and VPA+MMP-9 MO) < 0.0001*] (Fig. 3B). The maximal excitatory responses were not significantly different for only control

MO and MMP-9 MO groups *[Total charge (pA.sec): control MO, 2926.95 ± 994.03, n = 8; MMP-9 MO, 2295.82 ± 478.24, n = 9, p (control MO and MMP-9 MO) = 0.56*] (Fig. 3C). The VPA+MMP-9 MO group showed decreased frequency of barrages compared to the VPA +control MO group, suggesting that the downregulation of MMP-9 using MMP-9 MO rescues VPA-induced effects on spontaneous network activity [*Number of barrages: VPA+control MO, 1.88 ± 0.56, n = 9; VPA+MMP-9 MO, 0.7 ± 0.3, n = 10*]. The number of barrages were similar in only control MO and MMP-9 MO groups in the absence of VPA exposure [*control MO, 1.09 ± 0.31, n = 11; MMP-9 MO, 1.22 ± 0.31, n = 18*] (Fig. 3D). Consistent with the SB-3CT findings, these data suggest that suppressing VPA-induced MMP-9 elevations, results in a reversal of VPA effects on excitatory synapse overconnectivity, but has little effect on baseline transmission in untreated animals.

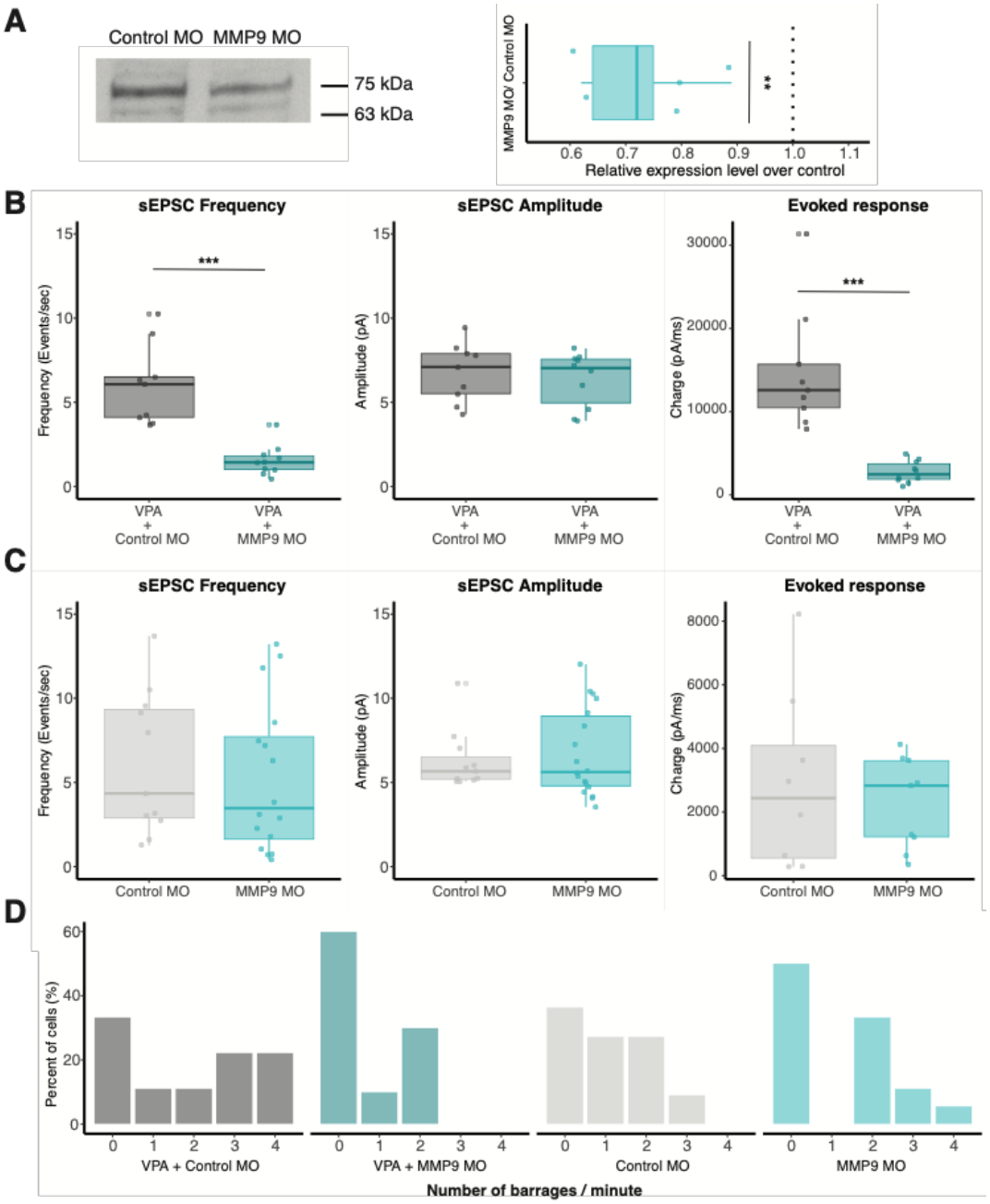

Figure 3: Morpholino targeted against MMP-9 rescues VPA-induced effects.

A. Western blot image (left) indicating MMP-9 levels (75kD band) in control (scrambled) MO and MMP-9 MO transfected groups. Boxplot (right) shows relative MMP-9 levels for control MO and MMP MO transfected tadpoles. MMP-9 MO group consistently shows relatively reduced MMP-9 levels compared to controls. The dotted line represents a ratio of 1 (no difference). The 63kDa band is a non-specific band labelled by MMP-9 antibody that shows no change. **B.** Boxplots showing sEPSC frequency, amplitude and evoked synaptic response from VPA + Control MO and VPA + MMP-9 MO groups. Frequency of sEPSCs and not amplitude are significantly enhanced in VPA + control MO group. Total charge from evoked synaptic response is significantly higher in the VPA + Control MO compared to VPA + MMP-9 MO treated animals. Data are represented as median ± IQR. **C.** Boxplots showing sEPSC frequency, amplitude and evoked synaptic response from Control MO and MMP-9 MO alone. Control MO and MMP-9 MO alone does not differ significantly in sEPSC frequency or amplitude. MMP-9 MO alone does not show any significant effect on evoked response. Data are represented as median ± IQR. **D.** Histogram showing relative barrage frequency for each group. Higher number of barrages are observed for VPA + control MO, and this effect is rescued by addition of MMP-9 MO. ** $p < 0.005$, *** $p < 0.0001$.

Inhibition of MMP-9 reverses VPA-induced behavioral effects

The results so far suggest that increasing levels of MMP-9 produces VPA-like hyperconnected excitable tectal networks while downregulation of MMP-9 rescues these effects. One consequence resulting from increased recurrent circuitry within the tectum, and possibly other brain regions, is that this circuitry can promote the generation of behaviors associated with hyperexcitability like increased seizure susceptibility or abnormal startle habituation response(James et al., 2015). We tested whether inhibition of MMP-9 could reverse these behavioral effects of VPA. To measure seizure susceptibility, tadpoles were exposed to 5mM of the convulsant PTZ, over a period of 20 minutes, during which seizure activity was characterized. One-way ANOVA revealed significant differences for seizure frequency across different treatment groups [*seizure frequency (events/minute): $p = 0.01$; time to first seizure (s): $p = 0.006$*]. Consistent with prior work, VPA-reared tadpoles exhibited more frequent pharmacologically induced seizures compared to their matched controls, while animals reared in VPA+SB-3CT showed no increased seizure frequency, that is, a reversal of the VPA-induced effect [*seizure frequency (events/minute): control, 0.72 ± 0.04, $n = 48$; VPA, 0.90 ± 0.04, $n = 45$; VPA+SB-3CT, 0.8 ± 0.05, $n = 34$; p(control and VPA) $= 0.004$; p(VPA and VPA+SB-3CT) $= 0.12$*] (Fig. 4A). This indicates that pharmacologically inhibiting MMP-9 during VPA exposure prevents VPA-induced changes in seizure susceptibility. As a second behavioral test, we measured acoustic startle habituation responses by presenting a repeated acoustic stimuli over six bouts. Typically, tadpoles show habituation during each bout and across bouts(James et al., 2015). A repeated measure ANOVA revealed significant differences in startle speed across experimental groups [*$p < 0.001$], bouts [$p < 0.001$] and group*bouts [$p < 0.001$*] interaction. Control tadpoles showed decreased startle speed over repeated bouts; indicating habituation (Fig. 4B). In VPA reared tadpoles, the animals showed reduced habituation. Co-exposure of SB-3CT and VPA reversed VPA-induced effects; although the startle habituation was significantly, but only

partially restored relative to control levels. The sixth bout was measured with a 15 minute delay between bouts, indicating long-term habituation, and this was also similarly affected across experimental groups.

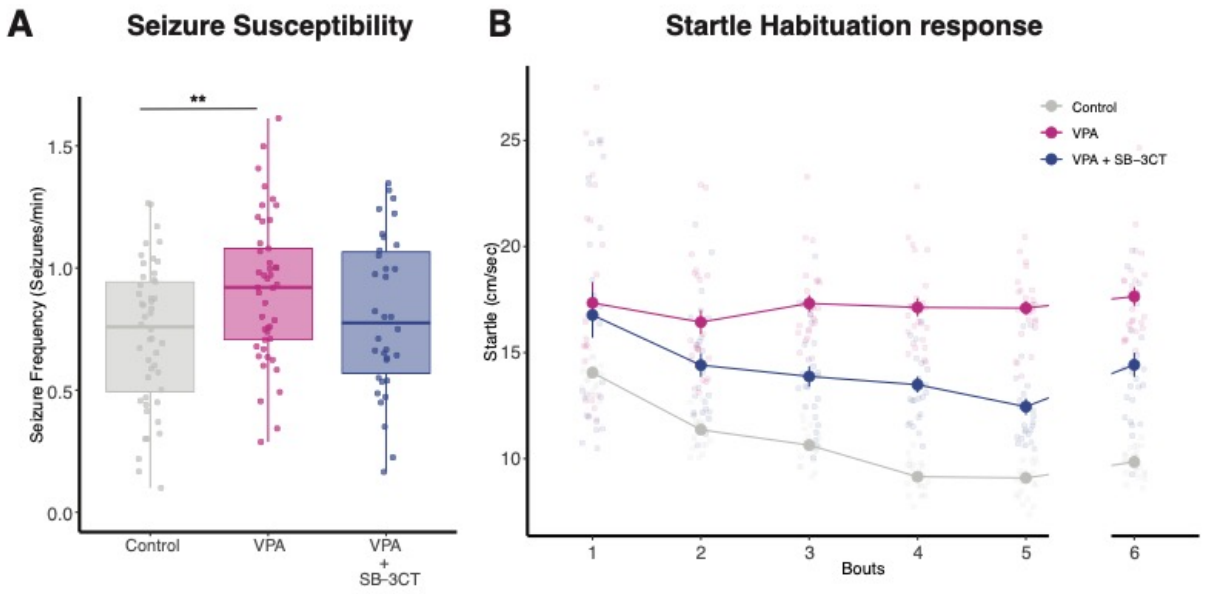

Figure 4: Inhibition of MMP-9 reverses VPA-induced behavioral effects

A. Boxplots showing seizure frequencies for Control, VPA and VPA + SB-3CT groups. Seizure frequency is increased in the VPA group, but this effect is rescued by addition of SB-3CT. Data are represented as median ± IQR. **B.** Line plot for startle response habituation for Control, VPA and VPA + SB-3CT. VPA-treated animals show less habituation to startle response compared to control animals. Addition of SB-3CT to VPA reverses this effect. Bouts 1 to 5 are separated by 5 min time intervals, whereas bout 6 is separated from bout 5 by a 15 min time interval. Each dot represents average with standard error bars. ** $p < 0.005$.

Enhanced visual activity increases MMP-9 levels and MMP-9 inhibition prevents visual-activity induced dendritic growth

Our data suggest that while inhibiting MMP-9 reverses the effect of VPA, this inhibition has no effect on control animals, suggesting that MMP-9 levels are basaly low. One possibility is that during normal development, MMP-9 levels are tightly regulated by neural activity and are elevated transiently when there is a need for structural plasticity. Thus, periods of increased MMP-9 activity may correlate with

experience-dependent synaptic reorganization during critical periods in the development of an organism(Murase et al., 2017). We used an assay for experience-dependent plasticity in the tectum, to test this hypothesis. Exposure of freely-swimming tadpoles to enhanced-visual stimulation for several hours is known to promote tectal neuron dendritic growth and synaptogenesis(Aizenman & Cline, 2007; Sin et al., 2002). We first tested whether this manipulation elevated MMP-9 levels in the brain. We exposed a group of tadpoles to enhanced visual activity in a custom-built chamber for 4 hours, another group was dark-exposed and a third group was left in normal light/dark rearing conditions, and then measured brain MMP-9 levels using a Western blot. We found that exposure to enhanced visual activity resulted in significantly increased MMP-9 levels compared to dark and normal rearing conditions *[Ratio of MMP-9 levels: L/D, 1.34 ± 0.10, n = 5; L/N, 1.35 ± 0.10, n = 5; D/N, 1.04 ± 0.14, n = 5; p (L/D) = 0.03; p (L/N) = 0.03; p (D/N) = 0.79*) (Figure 5A, B). We then compared the effect of MMP-9 inhibition on visual-stimulation induced dendritic growth. We used electroporation to express GFP in single tectal neurons *in vivo(Bestman et al., 2006)*, and then imaged and reconstructed dendritic arbors to compare dendritic growth rate during a 3 hour dark-exposure period vs. growth rate after 3 hours of enhanced visual stimulation. We observed that in the control group, enhanced visual stimulation results in an increase in the total dendritic branch length compared to the dark period [*Growth of total dendritic length (percent): Control/Dark, 97.35 ± 5.76, n = 9; Control/Light, 128.32 ± 7.25, n = 9*] (Fig. 5C). In the presence of SB-3CT, the enhanced visual stimuli does not increase total dendritic branch length [*Growth of total dendritic length (%): SB-3CT/Dark, 107.30 ± 6.61, n = 9; SB-3CT/Light, 96.88 ± 7.88, n =9*]. Thus, the change in dendritic growth rate was significantly decreased in the SB-3CT reared tadpoles in comparison to the matched control animals [*Change in growth rate (%): Control, 136.61 ± 12.29, n = 9; SB-3CT, 91.27 ± 6.42, n = 9; p = 0.009*] (Fig. 5D, E). Taken together, these results suggest that enhanced visual stimulation increased MMP-9 levels, and that this increase is necessary for

proper activity-driven dendritic arborization. By extension, chronically elevated levels of MMP-9 present in VPA treated tadpoles would result in unregulated plasticity, leading to hyperconnectivity and hyperexcitability.

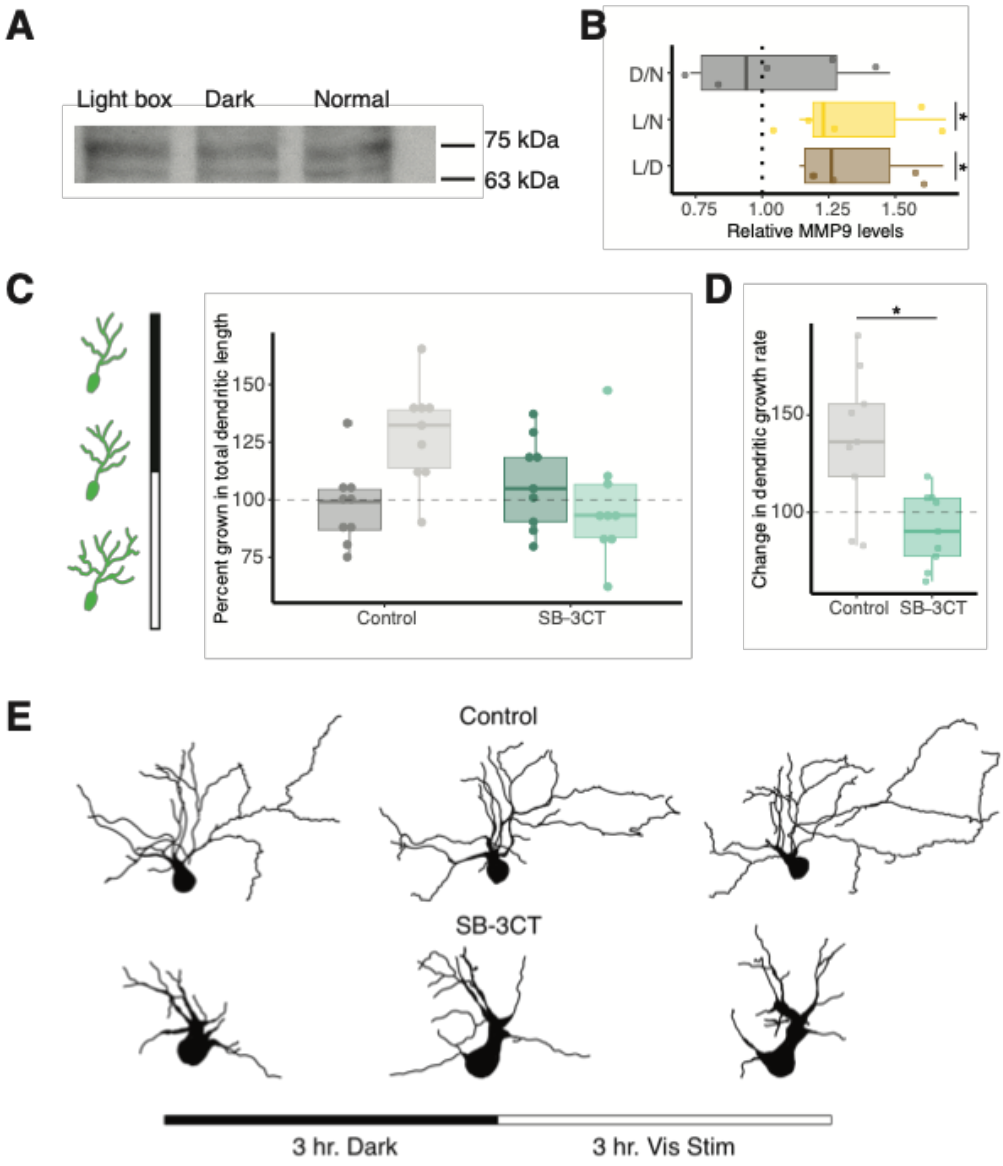

Figure 5: Enhanced visual activity increases MMP-9 levels and MMP-9 inhibition prevents visual-activity induced dendritic growth.

A. Western blot analysis specifying MMP-9 levels (75 kDa band) after lightbox, dark exposure and naive controls (normal). **B.** Box plot showing relative MMP-9 levels for light box treatment (enhanced visual stimulation) vs dark exposed (L/D), light box vs naive controls (L/N) and dark exposed vs naive controls (D/N), based on Western blot analysis. Enhanced visual activity using a light box experimental setup significantly increases relative MMP-9 levels compared to dark and normal rearing conditions. The dotted line represents a ratio of 1 (no difference). Data are represented as median ± IQR. **C.** Left panel shows schematic of experimental design, three confocal imaging sessions were performed: one at the start of an experiment, a second after 3 hours of dark exposure and a third after 3 hours of enhanced visual stimulation. In control animals, visual stimulation enhances dendritic growth whereas SB-3CT prevents dendritic growth during this period. **D.** SB-3CT significantly reduces the growth rate of dendrites during visual stimulation compared to the control group. Data are represented as median ± IQR. **E.** Representative 2D tracings of 3D tectal cell reconstructions from control and SB-3CT groups are shown before any treatment (left), after 3 hours of dark exposure (middle) and after enhanced visual stimulation (right). * $p < 0.05$.

Discussion

The results of this study suggest that chronic MMP-9 upregulation during early exposure to VPA, is responsible for mediating its effects on neural circuit connectivity and behavior. Exposure to VPA during a key developmental period in Xenopus produces hyperconnected and hyperexcitable neural networks responsible for producing abnormal behaviors such as enhanced seizure susceptibility and decreased habituation(James et al., 2015). Similarly, we found that upregulation of MMP-9 via overexpression resulted in increased frequency of sEPSCs, sIPSCs and barrages suggesting increased tectal connectivity and excitability. Downregulation of MMP-9 not only reversed VPA-induced synaptic connectivity and excitability in developing Xenopus tectum but also rescued VPA-induced behavioral effects. This suggests that chronically elevated levels of MMP-9 may produce abnormally high and sustained plasticity, leading to overconnectivity. Sensory experience during critical periods of development is crucial for proper maturation of sensory networks, and may involve transient, activity-dependent increases in MMP-9. In *Xenopus*, acute exposure to enhanced visual activity results in increased plasticity and dendritic growth in optic tectal neurons(Aizenman & Cline, 2007; Sin et al., 2002). We found that following enhanced visual stimulation, MMP-9 levels were elevated and that increased MMP-9 was necessary for experience-dependent dendritic growth, suggesting that during normal development, MMP-9 levels are low but transiently elevated to facilitate activity-induced structural plasticity.

MMP-9 plays a paramount role in establishing synaptic connections during development and in restructuring of synaptic networks in the adult brain(Reinhard et al., 2015). Recent studies show that MMP-mediated proteolysis is important for remodelling of synaptic structure and function required for processes such as learning and memory, and action of MMPs on various extracellular matrix components, cell surface receptors and growth factors is crucial for modulating neurogenesis and neuroplasticity(Huntley, 2012). Dysregulated expression and activity of MMP-9 can result in abnormal

synaptic remodelling; a hallmark of various neurodevelopmental disorders(Huntley, 2012). In particular, dysregulation of MMP-9 is known to influence cognitive processes(Beroun et al., 2019) and increased MMP-9 levels are associated with several neurodevelopmental disorders including ASD(Abdallah et al., 2012; Yoo et al., 2016), fragile X syndrome(Dziembowska et al., 2013; Sidhu et al., 2014), epilepsy(Konopka et al., 2013), bipolar disorder(Rybakowski et al., 2013) and schizophrenia.(Yamamori et al., 2013). Consistent with these studies, our data showed that elevated MMP-9 activity results in neurodevelopmental deficits in Xenopus by creating a hyperplastic state which leads to local overconnectivity.

Early life sensory experience during critical periods of development modifies functional circuits in the brain(Chklovskii et al., 2004; Hensch & Fagiolini, 2005). Periods of high MMP-9 activity correlate with structural and functional synaptic reorganization during critical period plasticity (CPP) and developmental windows across CNS regions, suggesting a role for MMP-9 in determining the developmental time course of CPP(Kaliszewska et al., 2012; Oliveira-Silva et al., 2007; Spolidoro et al., 2012). The results from our study are consistent with these observations in that MMP-9 levels increase in response to enhanced visual activity during a key period of development. Furthermore, this increase in MMP-9 correlates with visual activity induced plasticity and the inhibition of MMP-9 using a pharmacological inhibitor prevents visual-activity induced dendritic growth. The secretion and activation of MMP-9 is tightly regulated by a wide variety of factors and once activated, it can act on multiple targets including various components of the ECM, cell adhesion molecules, cell surface receptors, cytokines, growth factors, and other proteases, each of which can have differential effects in creating permissive environments for structural plasticity in the brain(Van den Steen et al., 2002; Vandooren et al., 2013).

This central role for MMP-9 is further supported by recent studies in adult mice, in which upon light reintroduction, intense MMP-9 activity is observed surrounding excitatory synapses in the binocular visual cortex suggesting that MMP-9 can modulate plasticity even after closure of critical periods(Murase et al., 2017, 2019). Enzymatic activity of MMP-9 has been known for inducing and maintaining long term potentiation and causes elongation and thinning of dendritic spines in the hippocampal neurons(Huntley, 2012; Michaluk et al., 2011). MMP-9 knock-out mice and overexpressing models show significantly reduced synaptic plasticity suggesting that appropriate levels of MMP-9 are needed for structural and functional reorganization of the brain(Wiera et al., 2013). Local activation of MMP-9 at the level of individual synapses can induce the maturation of spine heads(Szepesi et al., 2014). MMP-9 can act on various cell surface receptors like integrins, BDNF, ICAMs, NGL, all of which are known to be important for developmental and adult plasticity(Fiore et al., 2002; H. Lee et al., 2014; Michaluk et al., 2009; Yamamori et al., 2013). MMP-9, through activation of cell surface and cell adhesion molecules, is implicated not only in active dendritic spine remodeling and stabilization but also in pre- and postsynaptic receptor dynamics; consolidation of LTP; myelination and synaptic pruning(Reinhard et al., 2015). Perineuronal nets (PNNs), which are extracellular matrix components, are often associated with inhibitory interneurons and regulate their development and functions. Recent studies have shown that MMP-9 can rapidly degrade the PNNs surrounding various neurons enabling synaptic and network reorganization during experience dependent plasticity, and could also provide a mechanism by which dysregulation of MMP-9 can lead to abnormal development of neural circuitry(Murase et al., 2017, 2019; Wen et al., 2018).

Thus, understanding the precise downstream targets and functions of MMP-9 will be critical for understanding various cellular and molecular mechanisms underlying neurodevelopmental

disorders. Our study highlights the importance of MMP-9 in the etiology of neurodevelopmental disorders and future studies will focus on investigating the downstream molecular targets of MMP-9.

Materials and Methods

All animal experiments were performed in accordance with and approved by Brown University Institutional Animal Care and Use Committee standards and guidelines (Protocol number 19-05-0016).

Experimental animals

All experimental comparisons were done with matched controls from the same clutch, to account for variability in responses over time and across experimental groups.

Drug treatments

Tadpoles were raised in Steinberg's rearing media on a 12 h light/dark cycle at 18–21°C for 7–8 d, until they reached developmental stage 42(Nieuwkoop & Faber, 1958). They were then transferred to either (i) control rearing media, (ii) 1 mM solution of VPA in Steinberg's solution, (iii) 1 mM VPA + 3 uM SB-3CT (a pharmacological inhibitor of MMP-9) or (iv)3 uM SB-3CT alone, depending on the experiment, and raised at temperatures ranging from 18°C to 21°C until they reached developmental stages of either 47-48. Developmental stages of tadpoles were determined according to Nieuwkoop and Faber (1958). For all the electrophysiological and behavioral experiments the same concentration of VPA and SB-3CT were used. Previous experiments utilizing 1 mM VPA elicited distinct electrophysiological and behavioral effects(James et al., 2015). The rearing medium was renewed every 3 d. Animals of either sex were used because, at these developmental stages, tadpoles of either sex are phenotypically indistinguishable.

Plasmid and antisense constructs:

MMP-9 overexpression construct: The MMP-9 overexpression plasmid contained a backbone of pCMV-SPORT6 plasmid with CMV promoter driving the expression of downstream cloned genes - MMP-9 and a GFP reporter. GFP control construct: The GFP control plasmid consisted of a backbone of pCMV-SPORT6 plasmid with CMV promoter driving the expression of only a GFP reporter. Each working solution contained 4ug/ul of appropriate overexpression plasmid + 0.3uL Fast Green.

Reduction of matrix metalloproteinase 9 gene expression was accomplished through electroporation of a morpholino antisense oligonucleotide (MO)(Bestman & Cline, 2014). Lissamine tagged MOs were designed and ordered from GeneTools. Sequences used for the MMP-9 MO and control MO were 5' AGACTAAAACTCCCACCCTACCCAT 3' and 5' CCTCTTACCTCAGTTACAATTTATA 3', respectively, and were adopted from the methods of Faulkner *et al*. (2014). The control MO was a scrambled MO not known to align elsewhere. Working solution was prepared by diluting stock MO using endotoxin free molecular grade water and adding 1% Fast Green stock solution to make up 6% of the working solution, with a final concentration of 0.1mM of MO.

Tectal cell transfection:

To transfect cells in the tectum, stage 43-44 animals were anesthetized in a solution of 0.01% MS-222, plasmids or antisense morpholino constructs were injected into the midbrain ventricle, and voltage pulses were applied across the midbrain using platinum electrodes to electroporate cells lining the tectal ventricle(Haas et al., 2002). Tadpoles were then screened for appropriate transfection by checking for fluorescence under a fluorescence microscope.

Behavioral assays

Tadpoles that were used for seizures and acoustic startle response habituation protocols were not used again for other experiments. Immediately before behavioral experiments, tadpoles were transferred to Steinberg's media and left for 1 h to recover from acute action of the drug.

Seizures

For seizure experiments, when tadpoles reached stage 47, they were transferred into individual wells in a six-well plate (Corning), each filled with 7 ml of 5 mm pentylenetetrazol (PTZ) solution in Steinberg's media. The plate was diffusely illuminated from below and an overhead SCB 2001 color camera (Samsung) imaged tadpoles at 30 frames/s. Tadpole positions were acquired using Noldus EthoVision XT (Noldus Information Technology) and processed offline in a custom MATLAB program (MathWorks). Seizure events were defined as periods of rapid and irregular movement, interrupted by periods of immobility (Bell et al., 2011) The onset of regular seizures happened on average 3.9 ± 1.3 min into the recording and were detected automatically using swimming speed thresholding at a level of half of the maximal swimming speed. Number, frequency and duration of seizure events were measured across 5 min intervals of a 20-min-long recording.

Startle habituation response

A six-well plate fixed between two audio speakers (SPA2210/27; Philips), and mechanically connected to diaphragms of these speakers by inflexible plastic struts acted as an experimental arena for the startle habituation response experiment. Stage 49 tadpoles were placed in the experimental arena and acoustic stimuli (one period of a 200 Hz sine wave, 5 ms long) were presented every 5 s which evoked a reliable startle response. The observed startle response is likely due to a combination of inner ear-mediated and lateral line-mediated inputs, and, for the purposes of this study, we did not attempt to differentiate between the two. The amplitude of stimuli for habituation experiments was set at two times above the

startle threshold. Each train of stimuli lasted for 2 min; trains 1 to 5 were separated by 5 min gaps, whereas train 6 was separated from train 5 by a 15 min gap. In order to compensate for possible variation in stimulus delivery across the wells, the location of treatment (1 mM VPA and 1 mM VPA + 3 uM SB-3CT) tadpoles and matched controls within the six-well plate was alternated across experiments. An overhead camera was used to acquire videos of the tadpoles, which were then tracked in EthoVision and processed offline in a custom MATLAB script. Peak speed of each startle response was measured across a 2 s interval after stimulus delivery. To quantify habituation of startle responses at different timescales, we adopted the nomenclature from previous studies(Eddins et al., 2010)(Roberts et al., 2011). Startle speeds were averaged across 1-min-long periods of acoustic stimulation and compared across periods. For rapid habituation, we compared responses during minutes 1 and 2 of the first 2-min train of stimuli.

Electrophysiology experiments

For whole-brain recordings, tadpole brains were prepared as described by Wu et al. (1996) and Aizenman et al. (2003). In brief, tadpoles were anesthetized in 0.02% tricainemethane sulfonate (MS-222). To access the ventral surface of the tectum, brains were filleted along the dorsal midline and dissected in HEPES-buffered extracellular saline [in mm: 115 NaCl, 2 KCl, 3 Cacl2, 3 MgCl2, 5 HEPES, 10 glucose, pH 7.2 (osmolarity, 255 mOsm)]. Brains were then pinned to a submerged block of Sylgard in a recording chamber and maintained at room temperature (24°C). To access tectal cells, the ventricular membrane surrounding the tectum was carefully removed using a broken glass pipette. For evoked synaptic response experiments, a bipolar stimulating electrode (FHC) was placed on the optic chiasm to activate RGC axons.

Whole-cell voltage-clamp and current-clamp recordings were performed using glass micropipettes (8–12 MΩ) filled with K-gluconate intracellular saline [in mm: 100 K-gluconate, 8 KCl, 5 NaCl, 1.5 MgCl2,

20 HEPES, 10 EGTA, 2 ATP, and 0.3 GTP, pH 7.2 (osmolarity, 255 mOsm)]. Recordings were restricted consistently to retinorecipient neurons in the middle one-third of the tectum, thus avoiding any developmental variability existing along the rostrocaudal axis (Wu et al., 1996; Khakhalin and Aizenman, 2012; Hamodi and Pratt, 2014). Electrical signals were measured with a Multiclamp 700B amplifier (Molecular Devices), digitized at 10 kHz using a Digidata 1440 analog-to-digital board, and acquired using pClamp 10 software. Leak subtraction was done in real time using the acquisition software. Membrane potential in the figures was not adjusted to compensate for a predicted 12 mV liquid junction potential. Data were analyzed using AxographX software. Spontaneous synaptic events were collected and quantified using a variable amplitude template (Clements and Bekkers, 1997). Spontaneous EPSCs (sEPSCs) were recorded at −45 mV (the reversal for chloride ions) whereas sIPSCs were collected in control media at 5 mV (the reversal for glutamatergic currents). For each cell, 60 s of spontaneous activity was recorded. For evoked synaptic response experiments, a bipolar stimulating electrode (FHC) was placed on the optic chiasm to activate RGC axons. Synaptic stimulation experiments were conducted by collecting EPSCs evoked by stimulating the optic chiasm at a stimulus intensity that consistently evoked maximal amplitude EPSCs. Polysynaptic stimulation experiments were performed by collecting EPSCs evoked by stimulating the optic chiasm at a stimulus intensity that evoked the maximal amplitude EPSC. Quantification of polysynaptic activity was calculated by measuring the total change in current over 100 ms time bins beginning at the onset of the evoked response. A spontaneous barrage was defined as a change in holding current of 10 or 20 pA intervals for a period of >200 ms(James et al., 2015). The sEPSC recordings were scanned carefully manually to detect and quantify the number of barrages observed for each of the experimental groups. Graphs show median and interquartile ranges (IQRs) as error bars, and data in the text shows the averages and SEs.

Real-time quantitative PCR analysis

For quantifying MMP9 expression levels, whole tecta were harvested at developmental stage 49 from tadpoles reared in control conditions or with 1mM VPA from stage 42. Sequences used for the MMP-9 forward and reverse primer were 5' TCATGGGATCTTTTGCTCGT 3' and 5' CCTTGGGTAGCCATTATCAA 3', respectively. Optic tecta were collected from 10 tadpoles for each group from 3 independent breedings and stored in RNAlater prior to the isolation of RNA by TRIzol extraction. SuperScript IV VILO first strand cDNA synthesis was then performed according to the manufacturer's protocol (Invitrogen). Real-time quantitative PCR (RT-qPCR) was performed by using Power SYBR Green master kit with an Applied Biosystems StepOnePlus according to standard manufacturer's protocols (ThermoFisher). Data were analyzed by the ΔΔCT relative quantification method using the housekeeper gene RSP13.

Quantification of MMP-9 protein levels

Western blots were used to examine the protein expression changes in the midbrain of the tadpoles under different visual experience conditions or the knockdown of MMP-9. To examine the specificity of MMP-9 morpholino, whole-brain electroporation was performed at stage 47 tadpoles with 0.4mM morpholino oligos and plasmid that expresses MMP-9 fused with flag peptide (1mg/ml), and the midbrain tissues were dissected 2 days later. To test the effect of morpholino on knocking down endogenous MMP-9 protein expression, whole-brain electroporation was performed at stage 47 tadpoles with 0.4mM morpholino oligos, and the mid-brain tissues were collected 2 days after electroporation. In order to test the effect of different visual experience conditions on MMP-9 protein expression, animals were reared under enhanced visual stimulation, dark or ambient light (12-hour enhanced visual stimulations/12-hour dark).

Tissues were homogenized in lysis buffer documented in Joukov et al. (2001; HEPES 100mM (pH 7.5), NaCl 200mM, EDTA 40mM, EGTA 4mM, NaF 100mM, β-glycerophosphate 20mM, sodium orthovanadate 2mM, Nonidet P-40 1%, Complete Protease Inhibitor mixture 1:50), and the protein concentration was measured with Bio-Rad DC Protein Assay kit. 20µg of lysate was loaded onto an in-house made 7% gel for electrophoresis. Proteins were transferred to a nitrocellulose membrane with Trans-Blot Turbo transfer system (BioRad). The membrane was incubated in 5% blotting reagent/0.1% Tween-20 (Sigma) in TBS for an hour for blocking, and then transferred to primary MMP-9 antibody solution (1:2k; EMO millipore ab19016) diluted in blocking solution and incubated overnight at 4°C. After three brief washes with 0.1% Tween-20 in TBS, membranes were transferred to goat anti-rabbit HRP-conjugated secondary antibody (BioRad), diluted in blocking solution for an hour at room temperature. The Pierce ECL western blot substrate (Thermo Fisher Scientific, 32209) was used to visualize labeling. For quantification analysis, different exposure periods were used for the same blots to avoid saturation, and total protein normalization using Ponceau S as a loading control (Romero-Calvo et al., 2010). The densitometric analysis of western blot and the total protein was performed using Gel Analyzer of ImageJ, and the data of MMP-9 protein expression were normalized against the total protein as a loading control. Staining using anti-MMP-9 antibodies often resulted in labelling some non-specific bands in addition to the 75 kDa band. Thus, MMP-9-flag overexpression was used in combination with anti-flag antibodies to confirm specificity of the MMP-9 MO and confirm location of MMP-9 band.

Neuronal morphology

To label single tectal cells, Stage 44–45 tadpoles were electroporated using the pCALNL–GFP plus pCAG–Cre plasmids (courtesy Ed Ruthazer, McGill University, Montreal, Quebec, Canada; Ruthazer et al., 2013) at a ratio of 5000:1 to limit coexpression to a very small subset of neurons. Approximately 3 days after electroporation (around developmental stages 48-49) the animals were screened to check for

successful fluorescence. Tadpoles were selected for those in which a single neuron in the tectum was expressing GFP and could be imaged clearly. A Zeiss LSM 800 Confocal Laser Scanning Microscope was used to image tadpoles containing labeled neurons. Prior to the experiment tadpoles were either immersed in control media or media containing SB3CT. Animals were then anesthetized in 0.02% MS-222 and imaged under the 40X water immersion objective. For each animal, the clearest, most isolated and identifiable cell in the tectum was imaged. Initially, a z-stack encompassing the cell body and the entire length of all neurites was taken for each animal (as the reference image). After these reference images were taken, the tadpoles were transferred to the rearing media (Control or 3uM SB3CT) and incubated in dark for 3 hours. The same cell that had been previously imaged was identified for each animal and imaged after the 3-hour dark exposure. The tadpoles were then put back into their respective wells and subjected to enhanced visual stimuli using a "light box" for 3 hours. The light box consisted of a chamber with 4x3 array of green LEDs attached to the ceiling. Each row of LEDs flashed for one second and was then followed by the adjacent row, until all four rows had flashed and a one second pause occurred. The cycle then started over, and was presented over a 3 hour period. After visual simulation, a third image was taken. Dendritic arbors of imaged neurons were reconstructed in 3D and analyzed using Neutube and Fiji software (respectively). The total path length of each image was measured. Then, using the series of three images taken for each cell, growth rate was calculated.

Statistical analyses

For all the data, averages and SEs are given in the text, whereas median values and interquartile range (IQR) are shown in the figures. Sample sizes were based on power analyses and known variability from prior work in our experimental system. No outliers were removed from the data analysis, however, data points that were above 1.5 times IQR may be indicated as outliers in some graphs for data presentation purposes and increased clarity. One-way ANOVA was used to compare differences between overall

values of the groups. Repeated measures ANOVA was used to compare differences between startle speed (cm/s) with treatment groups as between-subjects variables and bouts as a repeated measure to assess habituation response upon repeated stimulation. Student two-tailed t-test with unequal variances was used to assess differences in relative MMP-9 levels across different treatments. Differences were considered statistically significant at $p<0.05$, and significant results followed by bonferroni post-hoc pairwise comparisons. All statistical analyses were carried out in R (R v3.6.1, <http://www.R-project.org>) with supplementary installed packages 'readr','lsr', 'ggplot2', 'nlme', 'ez','dplyr', 'stats', and 'lme4', 'emmeans'.

Acknowledgments and author contributions:

We are grateful for valuable intellectual input from members of the Aizenman lab. We thank Phouangmaly Mimi Oupravanh and Virgilio Lopez for animal and lab care. This work was supported by a Brown University OVPR Seed Award, a Carney Institute RI Neuroscience New Frontiers Award, NSF GRFP (EJ), and NIH – NEI R01 EY027380. C.D.A. oversaw project and design, performed electrophysiology experiments, prepared manuscript; S.G. designed experiments, performed electrophysiology experiments, analyzed data, prepared figures, ran statistics and prepared the manuscript; E.J.J. performed electrophysiology experiments; J.J.P. performed the behavioral assays; L.C.H. and H.T.C. designed and performed western blot analysis for quantifying MMP-9 levels and designed morpholinos, and contributed to the writing; A.T. performed qPCR analysis for quantifying MMP9 expression levels; A.B. performed neuronal morphology experiments. We thank Dr. Ed Ruthazer (McGill University, Montreal, Quebec, Canada) for providing plasmid constructs for labelling a small subset of neurons.

Competing interests:

On behalf of all the authors, the corresponding author declares no competing interest.

References:

Abdallah, M. W., Pearce, B. D., Larsen, N., Greaves-Lord, K., Nørgaard-Pedersen, B., Hougaard, D. M., Mortensen, E. L., & Grove, J. (2012). Amniotic fluid MMP-9 and neurotrophins in autism spectrum disorders: an exploratory study. *Autism Research: Official Journal of the International Society for Autism Research*, *5*(6), 428–433.

Aizenman, C. D., & Cline, H. T. (2007). Enhanced visual activity in vivo forms nascent synapses in the developing retinotectal projection. *Journal of Neurophysiology*, *97*(4), 2949–2957.

Beroun, A., Mitra, S., Michaluk, P., Pijet, B., Stefaniuk, M., & Kaczmarek, L. (2019). MMPs in learning and memory and neuropsychiatric disorders. *Cellular and Molecular Life Sciences*, *76*(16), 3207–3228.

Bestman, J. E., & Cline, H. T. (2014). Morpholino Studies in Xenopus Brain Development. *Methods in Molecular Biology* , *2047*, 377–395.

Bestman, J. E., Ewald, R. C., Chiu, S.-L., & Cline, H. T. (2006). In vivo single-cell electroporation for transfer of DNA and macromolecules. *Nature Protocols*, *1*(3), 1267–1272.

Betancur, C. (2011). Etiological heterogeneity in autism spectrum disorders: more than 100 genetic and genomic disorders and still counting. *Brain Research*, *1380*, 42–77.

Betancur, C., & Coleman, M. (2013). Etiological Heterogeneity in Autism Spectrum Disorders. *The Neuroscience of Autism Spectrum Disorders*, 113–144.

Bromley, R. L., Mawer, G. E., Briggs, M., Cheyne, C., Clayton-Smith, J., García-Fiñana, M., Kneen, R., Lucas, S. B., Shallcross, R., Baker, G. A., & Liverpool and Manchester Neurodevelopment Group.

(2013). The prevalence of neurodevelopmental disorders in children prenatally exposed to antiepileptic drugs. *Journal of Neurology, Neurosurgery, and Psychiatry*, *84*(6), 637–643.

Butler, M. G. (2018). *The Identification of the Genetic Components of Autism Spectrum Disorders 2017*. MDPI.

Chklovskii, D. B., Mel, B. W., & Svoboda, K. (2004). Cortical rewiring and information storage. *Nature*, *431*(7010), 782–788.

Choi, S.-Y. (2018). Synaptic and circuit development of the primary sensory cortex. *Experimental & Molecular Medicine*, *50*(4), 13.

Christensen, J., Grønborg, T. K., Sørensen, M. J., Schendel, D., Parner, E. T., Pedersen, L. H., & Vestergaard, M. (2013). Prenatal Valproate Exposure and Risk of Autism Spectrum Disorders and Childhood Autism. *JAMA*, *309*(16), 1696–1703.

Croft, C., C., E., & Banerjee-Basu, S. (2011). *Genetic Heterogeneity of Autism Spectrum Disorders*.

Deeg, K. E., & Aizenman, C. D. (2011). Sensory modality–specific homeostatic plasticity in the developing optic tectum. *Nature Neuroscience*, *14*(5), 548–550.

Dong, W., Lee, R. H., Xu, H., Yang, S., Pratt, K. G., Cao, V., Song, Y.-K., Nurmikko, A., & Aizenman, C. D. (2009). Visual avoidance in Xenopus tadpoles is correlated with the maturation of visual responses in the optic tectum. *Journal of Neurophysiology*, *101*(2), 803–815.

Dziembowska, M., Pretto, D. I., Janusz, A., Kaczmarek, L., Leigh, M. J., Gabriel, N., Durbin-Johnson, B., Hagerman, R. J., & Tassone, F. (2013). High MMP-9 activity levels in fragile X syndrome are lowered by minocycline. *American Journal of Medical Genetics. Part A*, *161A*(8), 1897–1903.

Eddins, D., Cerutti, D., Williams, P., Linney, E., & Levin, E. D. (2010). Zebrafish provide a sensitive model of persisting neurobehavioral effects of developmental chlorpyrifos exposure: comparison

with nicotine and pilocarpine effects and relationship to dopamine deficits. *Neurotoxicology and Teratology*, *32*(1), 99–108.

Ethell, I. M., & Ethell, D. W. (2007). Matrix metalloproteinases in brain development and remodeling: Synaptic functions and targets. *Journal of Neuroscience Research*, *85*(13), 2813–2823.

Ferrer-Ferrer, M., & Dityatev, A. (2018). Shaping Synapses by the Neural Extracellular Matrix. *Frontiers in Neuroanatomy*, *12*, 40.

Fiore, E., Fusco, C., Romero, P., & Stamenkovic, I. (2002). Matrix metalloproteinase 9 (MMP-9/gelatinase B) proteolytically cleaves ICAM-1 and participates in tumor cell resistance to natural killer cell-mediated cytotoxicity. *Oncogene*, *21*(34), 5213–5223.

Fujioka, H., Dairyo, Y., Yasunaga, K.-I., & Emoto, K. (2012). Neural functions of matrix metalloproteinases: plasticity, neurogenesis, and disease. *Biochemistry Research International*, *2012*, 789083.

Ghodke-Puranik, Y., Thorn, C. F., Lamba, J. K., Leeder, J. S., Song, W., Birnbaum, A. K., Altman, R. B., & Klein, T. E. (2013). Valproic acid pathway: pharmacokinetics and pharmacodynamics. *Pharmacogenetics and Genomics*, *23*(4), 236–241.

Grove, J., Ripke, S., Als, T. D., Mattheisen, M., Walters, R. K., Won, H., Pallesen, J., Agerbo, E., Andreassen, O. A., Anney, R., Awashti, S., Belliveau, R., Bettella, F., Buxbaum, J. D., Bybjerg-Grauholm, J., Bækvad-Hansen, M., Cerrato, F., Chambert, K., Christensen, J. H., … Børglum, A. D. (2019). Identification of common genetic risk variants for autism spectrum disorder. *Nature Genetics*, *51*(3), 431–444.

Haas, K., Jensen, K., Sin, W. C., Foa, L., & Cline, H. T. (2002). Targeted electroporation in Xenopus tadpoles in vivo – from single cells to the entire brain. *Differentiation*, *70*(4-5), 148–154.

Hensch, T. K., & Fagiolini, M. (2005). Excitatory–inhibitory balance and critical period plasticity in developing visual cortex. *Progress in Brain Research*, 115–124.

Huntley, G. W. (2012). Synaptic circuit remodelling by matrix metalloproteinases in health and disease. *Nature Reviews. Neuroscience*, *13*(11), 743–757.

James, E. J., Gu, J., Ramirez-Vizcarrondo, C. M., Hasan, M., Truszkowski, T. L. S., Tan, Y., Oupravanh, P. M., Khakhalin, A. S., & Aizenman, C. D. (2015). Valproate-induced neurodevelopmental deficits in Xenopus laevis tadpoles. *The Journal of Neuroscience: The Official Journal of the Society for Neuroscience*, *35*(7), 3218–3229.

Kaliszewska, A., Bijata, M., Kaczmarek, L., & Kossut, M. (2012). Experience-Dependent Plasticity of the Barrel Cortex in Mice Observed with 2-DG Brain Mapping and c-Fos: Effects of MMP-9 KO. *Cerebral Cortex*, *22*(9), 2160–2170.

Kataoka, S., Takuma, K., Hara, Y., Maeda, Y., Ago, Y., & Matsuda, T. (2013). Autism-like behaviours with transient histone hyperacetylation in mice treated prenatally with valproic acid. *The International Journal of Neuropsychopharmacology / Official Scientific Journal of the Collegium Internationale Neuropsychopharmacologicum* , *16*(1), 91–103.

Kim, K. C., Kim, P., Go, H. S., Choi, C. S., Yang, S.-I., Cheong, J. H., Shin, C. Y., & Ko, K. H. (2011). The critical period of valproate exposure to induce autistic symptoms in Sprague-Dawley rats. *Toxicology Letters*, *201*(2), 137–142.

Konopka, A., Grajkowska, W., Ziemiańska, K., Roszkowski, M., Daszkiewicz, P., Rysz, A., Marchel, A., Koperski, L., Wilczyński, G. M., & Dzwonek, J. (2013). Matrix metalloproteinase-9 (MMP-9) in human intractable epilepsy caused by focal cortical dysplasia. *Epilepsy Research*, *104*(1-2), 45–58.

Kumar, S., Reynolds, K., Ji, Y., Gu, R., Rai, S., & Zhou, C. J. (2019). Impaired neurodevelopmental pathways in autism spectrum disorder: a review of signaling mechanisms and crosstalk. *Journal of Neurodevelopmental Disorders*, *11*(1), 10.

Lee, H., Lee, E.-J., Song, Y. S., & Kim, E. (2014). Long-term depression-inducing stimuli promote cleavage of the synaptic adhesion molecule NGL-3 through NMDA receptors, matrix metalloproteinases and presenilin/γ-secretase. *Philosophical Transactions of the Royal Society of London. Series B, Biological Sciences*, *369*(1633), 20130158.

Lee, R. H., Mills, E. A., Schwartz, N., Bell, M. R., Deeg, K. E., Ruthazer, E. S., Marsh-Armstrong, N., & Aizenman, C. D. (2010). Neurodevelopmental effects of chronic exposure to elevated levels of pro-inflammatory cytokines in a developing visual system. *Neural Development*, *5*(1), 2.

Markram, K., & Markram, H. (2010). The Intense World Theory – A Unifying Theory of the Neurobiology of Autism. *Frontiers in Human Neuroscience*, *4*.

Markram, K., Rinaldi, T., La Mendola, D., Sandi, C., & Markram, H. (2008). Abnormal Fear Conditioning and Amygdala Processing in an Animal Model of Autism. *Neuropsychopharmacology*, *33*(4), 901–912.

Mehta, M. V., Gandal, M. J., & Siegel, S. J. (2011). mGluR5-antagonist mediated reversal of elevated stereotyped, repetitive behaviors in the VPA model of autism. *PloS One*, *6*(10), e26077.

Michaluk, P., Mikasova, L., Groc, L., Frischknecht, R., Choquet, D., & Kaczmarek, L. (2009). Matrix metalloproteinase-9 controls NMDA receptor surface diffusion through integrin beta1 signaling. *The Journal of Neuroscience: The Official Journal of the Society for Neuroscience*, *29*(18), 6007–6012.

Michaluk, P., Wawrzyniak, M., Alot, P., Szczot, M., Wyrembek, P., Mercik, K., Medvedev, N., Wilczek, E., De Roo, M., Zuschratter, W., Muller, D., Wilczynski, G. M., Mozrzymas, J. W.,

Stewart, M. G., Kaczmarek, L., & Wlodarczyk, J. (2011). Influence of matrix metalloproteinase MMP-9 on dendritic spine morphology. *Journal of Cell Science*, *124*(Pt 19), 3369–3380.

Moldrich, R. X., Leanage, G., She, D., Dolan-Evans, E., Nelson, M., Reza, N., & Reutens, D. C. (2013). Inhibition of histone deacetylase in utero causes sociability deficits in postnatal mice. *Behavioural Brain Research*, *257*, 253–264.

Murase, S., Lantz, C. L., & Quinlan, E. M. (2017). Light reintroduction after dark exposure reactivates plasticity in adults via perisynaptic activation of MMP-9. *Elife*, *6*, e27345.

Murase, S., Winkowski, D., Liu, J., Kanold, P. O., & Quinlan, E. M. (2019). Homeostatic regulation of perisynaptic matrix metalloproteinase 9 (MMP9) activity in the amblyopic visual cortex. *Elife*, *8*, e52503.

Niedringhaus, M., Chen, X., Dzakpasu, R., & Conant, K. (2012). MMPs and soluble ICAM-5 increase neuronal excitability within in vitro networks of hippocampal neurons. *PloS One*, *7*(8), e42631.

Nieuwkoop, P. D., & Faber, J. (1958). *Normal Table of Xenopus Laevis (Daudin)* (Vol. 1958, p. 65).

Oliveira-Silva, P., Jurgilas, P. B., Trindade, P., Campello-Costa, P., Perales, J., Savino, W., & Serfaty, C. A. (2007). Matrix Metalloproteinase-9 Is Involved in the Development and Plasticity of Retinotectal Projections in Rats. *Neuroimmunomodulation*, *14*(3-4), 144–149.

Peixoto, R. T., Kunz, P. A., Kwon, H., Mabb, A. M., Sabatini, B. L., Philpot, B. D., & Ehlers, M. D. (2012). Transsynaptic Signaling by Activity-Dependent Cleavage of Neuroligin-1. *Neuron*, *76*(3), 369–409.

Pielecka-Fortuna, J., Kalogeraki, E., Fortuna, M. G., & Löwel, S. (2015). Optimal level activity of matrix metalloproteinases is critical for adult visual plasticity in the healthy and stroke-affected brain. *eLife*, *5*, e11290.

Pratt, K. G., & Aizenman, C. D. (2007). Homeostatic regulation of intrinsic excitability and synaptic transmission in a developing visual circuit. *The Journal of Neuroscience: The Official Journal of the Society for Neuroscience*, *27*(31), 8268–8277.

Pratt, K. G., & Aizenman, C. D. (2009). Multisensory integration in mesencephalic trigeminal neurons in Xenopus tadpoles. *Journal of Neurophysiology*, *102*(1), 399–412.

Pratt, K. G., Dong, W., & Aizenman, C. D. (2008). Development and spike timing–dependent plasticity of recurrent excitation in the Xenopus optic tectum. *Nature Neuroscience*, *11*(4), 467–475.

Pratt, K. G., & Khakhalin, A. S. (2013). Modeling human neurodevelopmental disorders in the Xenopus tadpole: from mechanisms to therapeutic targets. *Disease Models & Mechanisms*, *6*(5), 1057–1065.

Reinhard, S. M., Razak, K., & Ethell, I. M. (2015). A delicate balance: role of MMP-9 in brain development and pathophysiology of neurodevelopmental disorders. *Frontiers in Cellular Neuroscience*, *9*.

Roberts, A. C., Reichl, J., Song, M. Y., Dearinger, A. D., Moridzadeh, N., Lu, E. D., Pearce, K., Esdin, J., & Glanzman, D. L. (2011). Habituation of the C-start response in larval zebrafish exhibits several distinct phases and sensitivity to NMDA receptor blockade. *PloS One*, *6*(12), e29132.

Rodier, P. M., Ingram, J. L., Tisdale, B., Nelson, S., & Romano, J. (1996). Embryological origin for autism: developmental anomalies of the cranial nerve motor nuclei. *The Journal of Comparative Neurology*, *370*(2), 247–261.

Roullet, F. I., Wollaston, L., Decatanzaro, D., & Foster, J. A. (2010). Behavioral and molecular changes in the mouse in response to prenatal exposure to the anti-epileptic drug valproic acid. *Neuroscience*, *170*(2), 514–522.

Rybakowski, J. K., Remlinger-Molenda, A., Czech-Kucharska, A., Wojcicka, M., Michalak, M., & Losy, J. (2013). Increased serum matrix metalloproteinase-9 (MMP-9) levels in young patients during bipolar depression. *Journal of Affective Disorders*, *146*(2), 286–289.

Schneider, T., & Przewłocki, R. (2005). Behavioral alterations in rats prenatally exposed to valproic acid: animal model of autism. *Neuropsychopharmacology: Official Publication of the American College of Neuropsychopharmacology*, *30*(1), 80–89.

Schneider, T., Turczak, J., & Przewłocki, R. (2006). Environmental enrichment reverses behavioral alterations in rats prenatally exposed to valproic acid: issues for a therapeutic approach in autism. *Neuropsychopharmacology: Official Publication of the American College of Neuropsychopharmacology*, *31*(1), 36–46.

Sidhu, H., Dansie, L. E., Hickmott, P. W., Ethell, D. W., & Ethell, I. M. (2014). Genetic Removal of Matrix Metalloproteinase 9 Rescues the Symptoms of Fragile X Syndrome in a Mouse Model. *Journal of Neuroscience*, *34*(30), 9867–9879.

Sin, W. C., Haas, K., Ruthazer, E. S., & Cline, H. T. (2002). Dendrite growth increased by visual activity requires NMDA receptor and Rho GTPases. *Nature*, *419*(6906), 475–480.

Spolidoro, M., Putignano, E., Munafò, C., Maffei, L., & Pizzorusso, T. (2012). Inhibition of Matrix Metalloproteinases Prevents the Potentiation of Nondeprived-Eye Responses after Monocular Deprivation in Juvenile Rats. *Cerebral Cortex*, *22*(3), 725–734.

Supekar, K., Uddin, L. Q., Khouzam, A., Phillips, J., Gaillard, W. D., Kenworthy, L. E., Yerys, B. E., Vaidya, C. J., & Menon, V. (2013). Brain Hyperconnectivity in Children with Autism and its Links to Social Deficits. *Cell Reports*, *5*(3), 738–747.

Szepesi, Z., Hosy, E., Ruszczycki, B., Bijata, M., Pyskaty, M., Bikbaev, A., Heine, M., Choquet, D., Kaczmarek, L., & Wlodarczyk, J. (2014). Synaptically released matrix metalloproteinase activity in

control of structural plasticity and the cell surface distribution of GluA1-AMPA receptors. *PloS One*, *9*(5), e98274.

Takarae, Y., & Sweeney, J. (2017). Neural Hyperexcitability in Autism Spectrum Disorders. *Brain Sci*, *7*(10).

Terbach, N., & Williams, R. S. B. (2009). Structure–function studies for the panacea, valproic acid. *Biochemical Society Transactions*, *37*(5), 1126–1132.

Truszkowski, T. L. S., James, E. J., Hasan, M., Wishard, T. J., Liu, Z., Pratt, K. G., Cline, H. T., & Aizenman, C. D. (2016). Fragile X mental retardation protein knockdown in the developing Xenopus tadpole optic tectum results in enhanced feedforward inhibition and behavioral deficits. *Neural Development*, *11*(1), 14.

Van den Steen, P. E., Dubois, B., Nelissen, I., Rudd, P. M., Dwek, R. A., & Opdenakker, G. (2002). Biochemistry and Molecular Biology of Gelatinase B or Matrix Metalloproteinase-9 (MMP-9). *Critical Reviews in Biochemistry and Molecular Biology*, *37*(6), 375–536.

Vandooren, J., Van den Steen, P. E., & Opdenakker, G. (2013). Biochemistry and molecular biology of gelatinase B or matrix metalloproteinase-9 (MMP-9): The next decade. *Critical Reviews in Biochemistry and Molecular Biology*, *48*(3), 222–272.

Wang, X.-B., Bozdagi, O., Nikitczuk, J. S., Zhai, Z. W., Zhou, Q., & Huntley, G. W. (2008). Extracellular proteolysis by matrix metalloproteinase-9 drives dendritic spine enlargement and long-term potentiation coordinately. *Proceedings of the National Academy of Sciences of the United States of America*, *105*(49), 19520–19525.

Wen, T. H., Afroz, S., Reinhard, S. M., Palacios, A. R., Tapia, K., Binder, D. K., Razak, K. A., & Ethell, I. M. (2018). Genetic Reduction of Matrix Metalloproteinase-9 Promotes Formation of Perineuronal

Nets Around Parvalbumin-Expressing Interneurons and Normalizes Auditory Cortex Responses in Developing Fmr1 Knock-Out Mice. *Cerebral Cortex* , *28*(11), 3951–3964.

Wiera, G., Wozniak, G., Bajor, M., Kaczmarek, L., & Mozrzymas, J. W. (2013). Maintenance of long-term potentiation in hippocampal mossy fiber-CA3 pathway requires fine-tuned MMP-9 proteolytic activity. *Hippocampus*, *23*(6), 529–543.

Yamamori, H., Hashimoto, R., Ishima, T., Kishi, F., Yasuda, Y., Ohi, K., Fujimoto, M., Umeda-Yano, S., Ito, A., Hashimoto, K., & Takeda, M. (2013). Plasma levels of mature brain-derived neurotrophic factor (BDNF) and matrix metalloproteinase-9 (MMP-9) in treatment-resistant schizophrenia treated with clozapine. *Neuroscience Letters*, *556*, 37–41.

Yoo, M. H., Kim, T.-Y., Yoon, Y. H., & Koh, J.-Y. (2016). Autism phenotypes in ZnT3 null mice: Involvement of zinc dyshomeostasis, MMP-9 activation and BDNF upregulation. *Scientific Reports*, *6*, 28548.